Journal of Sound and Vibration 326 (2009) 340–352

Contents lists available at ScienceDirect

Journal of Sound and Vibration

journal homepage: www.elsevier.com/locate/jsvi

Monitoring interfacial defects in a composite beam using impedance signatures

Wei Yan [a], J.B. Cai [b,*], W.Q. Chen [b]

[a] Faculty of Architectural, Civil Engineering and Environment, Ningbo University, Ningbo 315211, PR China
[b] Department of Civil Engineering, Zhejiang University, Hangzhou 310058, PR China

ARTICLE INFO

Article history:
Received 13 December 2008
Received in revised form
14 April 2009
Accepted 21 April 2009
Handling Editor: L.G. Tham
Available online 20 May 2009

ABSTRACT

A simply supported laminated beam bonded or embedded with a piezoelectric layer, which acts as sensor/actuator, is investigated using the state-space method. Linear spring-like constitutive relations are employed to model the behavior of interfacial bonding defects. The imperfect bonding between the host laminate and the piezoelectric transducer is also taken into account. Numerical results show that the electro-mechanical impedance (EMI) signatures extracted from the piezoelectric layer are very sensitive to the bonding imperfection of composite laminates. The covariance of the simulated data, which is a non-parametric damage index, is also employed to identify the severity of bonding imperfection quantitatively.

1. Introduction

Because of the excellent mechanical properties, low density and easy of shaping, laminated composites have been widely used in aerospace engineering, civil engineering, mechanical and even bioengineering [1]. Their integrity, especially in the interface region, is a very important factor in their life-time. Unfortunately, from a strictly physical point of view, the existence of a perfect interfacial bond in a real laminated composite seems impossible. Various flaws, such as microcracks, inhomogeneities and cavities, can be introduced into the bond in the process of fabrication. During the service lifetime, the structure will be subjected to various loads and exposed to corrosive environment. Consequently, these tiny flaws can get significant and finally lead to the local failure of bond. On the other hand, interfacial properties can strongly influence the behavior of the composites under thermal, mechanical and environmental conditions arising in service [2]. Thus, an ideal robust health monitoring scheme should be found to identify interfacial defects at a very early stage and provide some estimate of the extent or severity of the damage. However, due to the anisotropy of the material, the conductivity of the fibers, the insulative properties of the matrix and the fact that much of the damage often occurs beneath the top surface of the laminate, damage detection in composites is more difficult than in metallic structures [3].

Over the past decade, several techniques have been explored for detecting and monitoring of defects in composite materials. Adams et al. [4] showed that any defect in fiber-reinforced plastics could be detected by reduction in natural frequencies and increase in damping. Tan and Tong [5] detected a delamination in a laminated composite beam by monitoring the sensor charge output distributions along the beam of the first three-order frequencies. Kisa [6] investigated the effects of cracks on the dynamical characteristics of a cantilever composite beam. All of these investigations focus on damage detection in composite structures at low frequencies. Park et al. [7] presented an overview of impedance-based

* Corresponding author. Tel./fax: +86 571 88208475.
E-mail address: yanwei4467@163.com (J.B. Cai).

0022-460X/$ - see front matter © 2009 Elsevier Ltd. All rights reserved.
doi:10.1016/j.jsv.2009.04.030

health monitoring where the hardware and software issues are summarized, including a discussion of future research areas and the path forward. It can be shown that any change in the mechanical impedance, which could be caused by the presence of damage, will show up in the electrical impedance of the piezoelectric sensor. Although many investigations [8–10] indicated that this electro-mechanical impedance (EMI) technique is highly sensitive to detect minor changes in structural integrity using experimental measurement, due to the multiformity and complexity of the damage mechanisms of composite structures, we cannot predict their evolution through measurement only [11]. Thus, appropriate tools of simulation are necessary for monitoring system adapted to composite structures.

In order to establish an accurate EMI model for monitoring interfacial defects in composite beams, two important issues including the proper bonding imperfection simulation and dynamic analysis of a composite beam should be considered carefully. For a practical laminate, it is generally very difficult to predict the exact behavior of the interlaminar bonding theoretically. Some simplified interfacial models thus have been introduced. The most popular one is the linear spring-like model. For theoretical analysis, the interfacial tractions are continuous, while the displacements at either side of the interface layer become discontinuous. Micromechanics analysis shows that the jump in displacement is linearly proportional to the interfacial traction [12] and the proportional constants are the effective interface parameters (spring-like constant) [13,14]. For the accurate evaluation of behavior of intelligent structures, although the famous Pagano's exact solutions of a laminate in cylindrical bending [15,16] have been extended to include the piezoelectric coupling effect [17] and the interlaminar bonding imperfection [18,19], it should be pointed out that the exact elasticity analysis becomes computationally expensive when the number of layers in the laminate increases, because of a large number of integral constants that are involved. Note that the state-space method has been developed and proved to be particularly effective in analyzing laminated structures [20,21]. In this method, no matter how many layers are involved, the final solution scale remains the same and hence it is very powerful.

Surface bonded piezoelectric transducers are currently the most prominent area of research in damage detection using EMI signatures [22,23]. However, due to the durability and protection from surface finish, breakage and the corrosive environment, an embedded piezoelectric sensor and its interaction with the host composite structure have drawn much attention in the field of structural health monitoring (SHM) [24,25]. Thus, in this paper, a composite beam with either bonded or embedded piezoelectric layer is investigated based on the state-space formulations. A linear spring-like model is adopted to describe the behavior of interfacial defects including the imperfect bonding between the host laminate and the piezoelectric layer. Then, by virtue of the two-dimensional exact elasticity (piezoelasticity) equations and EMI model, an analytical expression of electrical admittance (inverse of the electrical impedance) related to the dynamics of the composite beam with imperfect interfaces is derived for SHM. Finally, numerical results are obtained and discussed to show the validity of the present analysis.

2. State-space method

For the application of EMI technique to SHM of laminated structures, a layered orthotropic beam bonded or embedded with a piezoelectric layer is considered, as shown in Fig. 1. For a beam structure, because the width is very thin and the load along the width stays invariant, the problem can be regarded as a plane-stress problem. In this case, the nonzero stress components are σ_x, σ_z and τ_{xz} only, which are independent of y. In the piezoelectric layers, there are additionally two nonzero electric displacement components D_x and D_z, which are also independent of y. Then we can derive the following two-dimensional constitutive relations [26]:

$$\sigma_x = \bar{c}_{11}\frac{\partial u}{\partial x} + \bar{c}_{13}\frac{\partial w}{\partial z} + \bar{e}_{31}\frac{\partial \phi}{\partial z}, \quad \sigma_z = \bar{c}_{13}\frac{\partial u}{\partial x} + \bar{c}_{33}\frac{\partial w}{\partial z} + \bar{e}_{33}\frac{\partial \phi}{\partial z},$$

$$\tau_{xz} = \bar{c}_{55}\left(\frac{\partial u}{\partial z} + \frac{\partial w}{\partial x}\right) + \bar{e}_{15}\frac{\partial \phi}{\partial x},$$

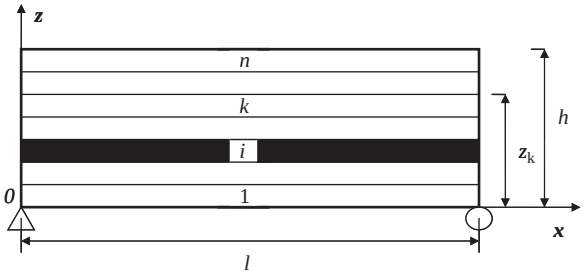

Fig. 1. Sketch of a composite beam with a piezoelectric layer.

$$D_x = \bar{e}_{15}\left(\frac{\partial u}{\partial z}+\frac{\partial w}{\partial x}\right)-\bar{\varepsilon}_{11}\frac{\partial \phi}{\partial x}, \quad D_z = \bar{e}_{31}\frac{\partial u}{\partial x}+\bar{e}_{33}\frac{\partial w}{\partial z}-\bar{\varepsilon}_{33}\frac{\partial \phi}{\partial z}, \tag{1}$$

where u and w are the displacement components in x and z directions, respectively. ϕ is the electric potential. $\bar{c}_{ij}$, $\bar{e}_{ij}$ and $\bar{\varepsilon}_{ij}$ are the reduced elastic, piezoelectric and dielectric constants, respectively, which are defined as follows:

$$\bar{c}_{11} = c_{11}-c_{12}^2/c_{22}, \quad \bar{c}_{13} = c_{13}-c_{12}c_{23}/c_{22}, \quad \bar{c}_{33} = c_{33}-c_{23}^2/c_{22},$$

$$\bar{c}_{55} = c_{55}, \quad \bar{e}_{31} = e_{31}-e_{32}c_{12}/c_{22}, \quad \bar{e}_{33} = e_{33}-e_{32}c_{23}/c_{22},$$

$$\bar{e}_{15} = e_{15}, \quad \bar{\varepsilon}_{11} = \varepsilon_{11}, \quad \bar{\varepsilon}_{33} = \varepsilon_{33}+e_{32}^2/c_{22}. \tag{2}$$

The equations of motion and Gaussian equation of electrostatics for the orthotropic piezoelectric layer are [26]

$$\frac{\partial \sigma_x}{\partial x}+\frac{\partial \tau_{xz}}{\partial z} = \rho\frac{\partial^2 u}{\partial t^2}, \quad \frac{\partial \tau_{xz}}{\partial x}+\frac{\partial \sigma_z}{\partial z} = \rho\frac{\partial^2 w}{\partial t^2}, \tag{3}$$

and

$$\frac{\partial D_x}{\partial x}+\frac{\partial D_z}{\partial z} = 0. \tag{4}$$

With a routine derivation, the following state equation can be obtained from Eqs. (1)–(4):

$$\frac{\partial}{\partial z}\begin{Bmatrix} u \\ \sigma_z \\ D_z \\ \tau_{xz} \\ w \\ \phi \end{Bmatrix} = \begin{bmatrix} 0 & 0 & 0 & \frac{1}{\bar{c}_{55}} & -\frac{\partial}{\partial x} & -\frac{\bar{e}_{15}}{\bar{c}_{55}}\frac{\partial}{\partial x} \\ 0 & 0 & 0 & -\frac{\partial}{\partial x} & \rho\frac{\partial^2}{\partial t^2} & 0 \\ 0 & 0 & 0 & -\frac{\bar{e}_{15}}{\bar{c}_{55}}\frac{\partial}{\partial x} & 0 & k_2\frac{\partial^2}{\partial x^2} \\ -k_1\frac{\partial^2}{\partial x^2}+\rho\frac{\partial^2}{\partial t^2} & -\beta_1\frac{\partial}{\partial x} & -\beta_2\frac{\partial}{\partial x} & 0 & 0 & 0 \\ -\beta_1\frac{\partial}{\partial x} & \frac{\bar{\varepsilon}_{33}}{\alpha} & \frac{\bar{e}_{33}}{\alpha} & 0 & 0 & 0 \\ -\beta_2\frac{\partial}{\partial x} & \frac{\bar{e}_{33}}{\alpha} & -\frac{\bar{c}_{33}}{\alpha} & 0 & 0 & 0 \end{bmatrix}\begin{Bmatrix} u \\ \sigma_z \\ D_z \\ \tau_{xz} \\ w \\ \phi \end{Bmatrix}, \tag{5}$$

in which

$$\alpha = \bar{c}_{33}\bar{\varepsilon}_{33}+\bar{e}_{33}^2, \quad \beta_1 = (\bar{c}_{13}\bar{\varepsilon}_{33}+\bar{e}_{31}\bar{e}_{33})/\alpha, \quad \beta_2 = (\bar{c}_{13}\bar{e}_{33}-\bar{c}_{33}\bar{e}_{31})/\alpha,$$

$$k_1 = \bar{c}_{11}-\bar{c}_{13}\beta_1-\bar{e}_{31}\beta_2, \quad k_2 = \bar{\varepsilon}_{11}+\bar{e}_{15}^2/\bar{c}_{55}, \quad \beta = \bar{c}_{11}-\bar{c}_{13}^2/\bar{c}_{33}. \tag{6}$$

The simply supported conditions are [26,27]

$$\sigma_x(0,z) = \sigma_x(l,z) = 0, \quad w(0,z) = w(l,z) = 0, \quad D_x(0,z) = D_x(l,z) = 0. \tag{7}$$

To satisfy these conditions, we assume

$$\begin{Bmatrix} u \\ \sigma_z \\ D_z \\ \tau_{xz} \\ w \\ \phi \end{Bmatrix} = \begin{Bmatrix} h\bar{u}(\zeta)\cos(m\pi\xi) \\ -\bar{c}_{11}^{(p)}\bar{\sigma}_z(\zeta)\sin(m\pi\xi) \\ -\sqrt{\bar{c}_{11}^{(p)}\bar{\varepsilon}_{33}^{(p)}}\bar{D}_z(\zeta)\sin(m\pi\xi) \\ \bar{c}_{11}^{(p)}\bar{\tau}_{xz}(\zeta)\cos(m\pi\xi) \\ h\bar{w}(\zeta)\sin(m\pi\xi) \\ h\sqrt{\bar{c}_{11}^{(p)}/\bar{\varepsilon}_{33}^{(p)}}\bar{\phi}(\zeta)\sin(m\pi\xi) \end{Bmatrix}\exp(\mathrm{i}\omega t), \tag{8}$$

where $\zeta = z/h$ and $\xi = x/l$ are dimensionless coordinates, the superscript "p" represents piezoelectric layer, a quantity with overbar except $\bar{c}_{11}^{(1)}$ indicates the dimensionless one and m is an integer. The substitution of Eq. (8) into Eq. (5) yields

$$\frac{\partial}{\partial \zeta}\mathbf{V}(\zeta) = \mathbf{A}\mathbf{V}(\zeta), \tag{9}$$

where

$$\mathbf{V}(\zeta) = [\bar{u}(\zeta)\ \ \bar{\sigma}_z(\zeta)\ \ \bar{D}_z(\zeta)\ \ \bar{\tau}_{xz}(\zeta)\ \ \bar{w}(\zeta)\ \ \bar{\phi}(\zeta)]^{\mathrm{T}} \tag{10}$$

and

$$\mathbf{A}=\begin{bmatrix} 0 & 0 & 0 & \dfrac{\bar{c}_{11}^{(p)}}{\bar{c}_{55}} & -k & -\dfrac{\bar{e}_{15}}{\bar{c}_{55}}\sqrt{\dfrac{\bar{c}_{11}^{(p)}}{\bar{\varepsilon}_{33}^{(p)}}}k \\ 0 & 0 & 0 & -k & \Omega^2\dfrac{\rho}{\rho^{(p)}} & 0 \\ 0 & 0 & 0 & -\dfrac{\bar{e}_{15}}{\bar{c}_{55}}\sqrt{\dfrac{\bar{c}_{11}^{(p)}}{\bar{\varepsilon}_{33}^{(p)}}}k & 0 & \dfrac{1}{\bar{\varepsilon}_{33}^{(p)}}k_2k^2 \\ \dfrac{k_1}{\bar{c}_{11}^{(p)}}k^2-\Omega^2\dfrac{\rho}{\rho^{(p)}} & \beta_1 k & \beta_2\sqrt{\dfrac{\bar{\varepsilon}_{33}^{(p)}}{\bar{c}_{11}^{(p)}}}k & 0 & 0 & 0 \\ \beta_1 k & -\dfrac{\bar{\varepsilon}_{33}\bar{c}_{11}^{(p)}}{\alpha} & -\dfrac{\bar{e}_{33}\sqrt{\bar{\varepsilon}_{33}^{(p)}\bar{c}_{11}^{(p)}}}{\alpha} & 0 & 0 & 0 \\ \beta_2\sqrt{\dfrac{\bar{\varepsilon}_{33}^{(p)}}{\bar{c}_{11}^{(p)}}}k & -\dfrac{\bar{e}_{33}\sqrt{\bar{\varepsilon}_{33}^{(p)}\bar{c}_{11}^{(p)}}}{\alpha} & \dfrac{\bar{c}_{33}\bar{\varepsilon}_{33}^{(p)}}{\alpha} & 0 & 0 & 0 \end{bmatrix}. \tag{11}$$

In the above equations, we have employed the following notations: $k=m\pi s$, $s=h/l$ (the thickness-to-span ratio) and $\Omega=\omega h\sqrt{\rho^{(p)}/\bar{c}_{11}^{(p)}}$ is the dimensionless angular frequency. The state equation for the elastic layers can be derived in a similar way and the corresponding state vector can be obtained by simply setting $e_{ij}=0$ in matrix $\mathbf{A}$ along with the deletion of the third and sixth rows and columns. The solution to Eq. (9) can be obtained as

$$\mathbf{V}(\zeta)=\exp[\mathbf{A}(\zeta-\zeta_{k-1})]\mathbf{V}(\zeta_{k-1}),\quad (\zeta_{k-1}\le\zeta\le\zeta_k,\ k=1,2,\ldots,n), \tag{12}$$

where $\zeta_0=0$, $\zeta_k=z_k/h=\sum_{j=1}^{k}h_j/h$ and h_k is the thickness of the kth layer.

Setting $\zeta=\zeta_k$ in Eq. (12), the relationship between the state variables at the upper and lower surfaces of the kth layer can be established

$$\mathbf{V}_1^{(k)}=\mathbf{M}_k\mathbf{V}_0^{(k)}, \tag{13}$$

where $\mathbf{V}_1^{(k)}$ and $\mathbf{V}_0^{(k)}$ are the state vectors at the upper and lower surfaces, respectively, of the kth layer and $\mathbf{M}_k=\exp[\mathbf{A}(\zeta_k-\zeta_{k-1})]$ is the transfer matrix. Similarly, we get

$$\mathbf{V}_1^{(k+1)}=\mathbf{M}_{k+1}\mathbf{V}_0^{(k+1)}. \tag{14}$$

In this paper, a spring-layer model is adopted to describe the interfacial imperfection [13,14]:

$$\sigma_z^{(k+1)}=\sigma_z^{(k)}=[w^{(k+1)}-w^{(k)}]/R_z^{(k)},\quad \tau_{xz}^{(k+1)}=\tau_{xz}^{(k)}=[u^{(k+1)}-u^{(k)}]/R_x^{(k)},\quad \text{at } \zeta=\zeta_k, \tag{15}$$

where $R_x^{(k)}$, $R_z^{(k)}$ are the compliance coefficients of the model. It is noted here that different values of compliance coefficients can be assigned, corresponding to different cases of bonding imperfections. For example, for the slip-type imperfection, we have $R_z^{(k)}=0$ while keeping $R_x^{(k)}$ as finite constants.

By virtue of Eq. (8), Eq. (15) can be rewritten in a matrix form as

$$\mathbf{V}_e^{(k+1)}(\zeta_k)=\mathbf{P}_k\mathbf{V}_e^{(k)}(\zeta_k), \tag{16}$$

in which $\mathbf{V}_e(\zeta)=[\bar{u}(\zeta)\ \ \bar{\sigma}_z(\zeta)\ \ \bar{\tau}_{xz}(\zeta)\ \ \bar{w}(\zeta)]^{\mathrm{T}}$ is the elastic part of state vector $\mathbf{V}(\zeta)$ and the subscript "e" means the transfer relation between the elastic state variable and the interfacial transfer matrix is

$$\mathbf{P}_k=\begin{bmatrix} 1 & 0 & \bar{R}_x^{(k)} & 0 \\ 0 & 1 & 0 & 0 \\ 0 & 0 & 1 & 0 \\ 0 & -\bar{R}_z^{(k)} & 0 & 1 \end{bmatrix}, \tag{17}$$

where $\bar{R}_x^{(k)}=\bar{c}_{11}^{(p)}R_x^{(k)}/h$, $\bar{R}_z^{(k)}=\bar{c}_{11}^{(p)}R_z^{(k)}/h$ are the dimensionless compliance coefficients in the spring-like model.

3. Electro-mechanical response of a composite beam with imperfect interfaces

3.1. A composite beam bonded with a surface piezoelectric layer

First, a composite beam bonded with a piezoelectric layer at the bottom surface is investigated. The relation between the state vectors at the top and bottom surfaces of the host elastic laminate can be derived from Eqs. (13), (14)

and (16),

$$\mathbf{V}_e^{(n)}(1) = \mathbf{T}_e \mathbf{V}_e^{(1)}(\zeta_1), \tag{18}$$

where $\mathbf{T}_e = \prod_{j=n}^{2} \mathbf{M}_e^{(j)} \mathbf{P}_{j-1}$ is the global transfer matrix for the elastic layers. The following mechanical and the electric boundary conditions of laminated beam are assumed:

$$\sigma_z^{(n)} = 0, \quad \tau_{xz}^{(n)} = 0, \quad \text{at } \zeta = 1,$$

$$\sigma_z^{(1)} = 0, \quad \tau_{xz}^{(1)} = 0, \quad D_z^{(1)} = 0, \quad \text{at } \zeta = 0, \tag{19-1}$$

and at the top surface of the piezoelectric actuator/sensor, we have

$$\phi = \phi_1 \exp(\mathrm{i}\omega t), \quad \text{at } \zeta = \zeta_1. \tag{19-2}$$

The applied electric potential can be expanded as

$$\phi_1 = h\sqrt{\bar{c}_{11}^{(p)}/\bar{\varepsilon}_{33}^{(p)}} \sum_{m=1}^{\infty} f_m \sin(m\pi\xi), \tag{20}$$

where $f_m = [2/(h\sqrt{\bar{c}_{11}^{(p)}/\bar{\varepsilon}_{33}^{(p)}})] \int_0^1 \phi_1 \sin(m\pi\xi)\,\mathrm{d}\xi$ are the Fourier coefficients. Then, for an arbitrary integer m, the following relation can be derived from Eqs. (13), (14) and (19):

$$\mathbf{V}_e^{(1)}(\zeta_1) = \mathbf{M}_e^{(1)} \mathbf{V}_e(0) + \mathbf{R}, \tag{21}$$

where

$$\mathbf{M}_e^{(1)} = \mathbf{M}_0^{(1)} - \frac{1}{m_{66}} \mathbf{L}_1 \mathbf{L}_2^{\mathrm{T}}, \quad \mathbf{R} = \frac{1}{m_{66}} \bar{\phi}_1 \mathbf{L}_1,$$

$$\mathbf{L}_1 = [m_{16} \;\; m_{26} \;\; m_{46} \;\; m_{56}]^{\mathrm{T}}, \quad \mathbf{L}_2 = [m_{61} \;\; m_{62} \;\; m_{64} \;\; m_{65}]^{\mathrm{T}}, \tag{22}$$

where m_{ij} are the elements of matrix $\mathbf{M}^{(1)}$; $\mathbf{M}_0^{(1)}$ is of order 4×4 that can be obtained by simply deleting the third and sixth rows as well as the third and sixth columns of $\mathbf{M}^{(1)}$. To calculate the state variables at any interior point, we need the following formulation:

$$\bar{\phi}_0 = \bar{\phi}(0) = \frac{1}{m_{66}} \bar{\phi}_1 - \frac{1}{m_{66}} [m_{61} \bar{u}(0) + m_{65} \bar{w}(0)]. \tag{23}$$

From Eqs. (18) and (21), we can get

$$\mathbf{V}_e^{(n)}(1) = \mathbf{T}\mathbf{V}_e(0) + \mathbf{Q}, \quad \mathbf{T} = \mathbf{T}_e \mathbf{M}_e^{(1)}, \quad \mathbf{Q} = \mathbf{T}_e \mathbf{R}. \tag{24}$$

By virtue of the mechanical boundary conditions in Eq. (19-1), we can get the following relation from Eq. (24):

$$\begin{bmatrix} \mathbf{T}_{21} & \mathbf{T}_{24} \\ \mathbf{T}_{31} & \mathbf{T}_{34} \end{bmatrix} \begin{Bmatrix} \bar{u}(0) \\ \bar{w}(0) \end{Bmatrix} = \begin{Bmatrix} \mathbf{Q}_{21} \\ \mathbf{Q}_{31} \end{Bmatrix}, \tag{25}$$

where $\mathbf{T}_{ij}$ and $\mathbf{Q}_{ij}$ are the corresponding elements of matrix $\mathbf{T}$ and the electrical load vector $\mathbf{Q}$, respectively. After the unknown state variables at the bottom surface are solved from Eqs. (25) and (23), the state vector at an arbitrary position can be calculated from Eq. (12).

3.2. A composite beam embedded with a piezoelectric layer

Then, a composite beam embedded with a piezoelectric layer is taken into account. The following boundary conditions at the top and bottom surfaces of laminated beam are assumed

$$\sigma_z^{(n)} = 0, \quad \tau_{xz}^{(n)} = 0, \quad \text{at } \zeta = 1,$$

$$\sigma_z^{(1)} = 0, \quad \tau_{xz}^{(1)} = 0, \quad \text{at } \zeta = 0. \tag{26}$$

Further, we assume that the ith layer of the laminated beam is the piezoelectric layer. At the top and bottom surfaces of the piezoelectric actuator/sensor, we have

$$D_z^{(i)} = 0, \quad \text{at } \zeta = \zeta_{i-1},$$

$$\phi = \phi_1 \exp(\mathrm{i}\omega t), \quad \text{at } \zeta = \zeta_i. \tag{27}$$

Then, the following relation can be derived from Eqs. (13), (14) and (27):

$$\mathbf{V}_e^{(i)}(\zeta_i) = \mathbf{M}_e^{(i)} \mathbf{V}_e(\zeta_{i-1}) + \mathbf{R}, \tag{28}$$

where

$$\mathbf{M}_e^{(i)} = \mathbf{M}_0^{(i)} - \frac{1}{m_{66}}\mathbf{L}_1\mathbf{L}_2^{\mathrm{T}}, \quad \mathbf{R} = \frac{1}{m_{66}}\bar{\phi}_1\mathbf{L}_1,$$

$$\mathbf{L}_1 = [m_{16}\ \ m_{26}\ \ m_{46}\ \ m_{56}]^{\mathrm{T}}, \quad \mathbf{L}_2 = [m_{61}\ \ m_{62}\ \ m_{64}\ \ m_{65}]^{\mathrm{T}}, \tag{29}$$

where m_{ij} are the elements of matrix $\mathbf{M}^{(i)}$; $\mathbf{M}_0^{(i)}$ is of order 4×4 that can be obtained by simply deleting the third and sixth rows as well as the third and sixth columns of $\mathbf{M}^{(i)}$. To calculate the state variables at any interior point, we also need the following formulation:

$$\bar{\phi}_0 = \bar{\phi}(\zeta_{i-1}) = \frac{1}{m_{66}}\bar{\phi}_1 - \frac{1}{m_{66}}\mathbf{L}_2^{\mathrm{T}}\mathbf{V}_e(\zeta_{i-1}). \tag{30}$$

Now the relation between the state vectors at the top and bottom surfaces of the elastic laminate can be derived from Eqs. (13), (14), (16) and (28):

$$\mathbf{V}_e^{(n)}(1) = \mathbf{T}\mathbf{V}_e(0) + \mathbf{Q}, \quad \mathbf{Q} = \mathbf{T}_1\mathbf{R}, \tag{31}$$

where $\mathbf{T} = (\prod_{j=n}^{2}\mathbf{M}_e^{(j)}\mathbf{P}_{j-1})\mathbf{M}_e^{(1)}$ is the global transfer matrix for the elastic variables and $\mathbf{T}_1 = (\prod_{j=n}^{i+1}\mathbf{M}_e^{(j)}\mathbf{P}_{j-1})$. Similarly, we have the following relation:

$$\begin{bmatrix}\mathbf{T}_{21} & \mathbf{T}_{24}\\ \mathbf{T}_{31} & \mathbf{T}_{34}\end{bmatrix}\begin{Bmatrix}\bar{u}(0)\\ \bar{w}(0)\end{Bmatrix} = \begin{Bmatrix}\mathbf{Q}_{21}\\ \mathbf{Q}_{31}\end{Bmatrix}. \tag{32}$$

It can be seen that all state variables including electric variables in the interior of the laminated beam (including piezoelectric layer) can be calculated by the above analysis.

4. Electro-mechanical impedance technique

As shown in Fig. 2, the piezoelectric layer can be divided into L segments and each segment is regarded as an impedance element. The L impedance elements are in parallel in the electric circuit and thus the electrical boundary conditions can be given as [28]

$$\bar{V}^{(1)} = \bar{V}^{(2)} \cdots = \bar{V}^{(L-1)} = \bar{V}^{(L)} = \bar{V}, \quad \bar{I} = \bar{I}^{(1)} + \bar{I}^{(2)} + \cdots + \bar{I}^{(L-1)} + \bar{I}^{(L)}, \tag{33}$$

in which a quantity with overbar indicates the dimensionless one. For an arbitrary impedance element j, the dimensionless electric current passing through the piezoelectric layer $\bar{I}^{(j)}$ can be determined as [23]

$$\bar{I}^{(j)} = \mathrm{i}\Omega\frac{\vartheta}{s}\int_0^1\int_{\xi_{j-1}}^{\xi_j}\bar{D}_z\,\mathrm{d}\xi\,\mathrm{d}\eta, \tag{34}$$

in which $\vartheta = b/h$, $s = h/l$, $\eta = y/b$, b is the width of composite beam. Because the composite beam is very narrow and the electric displacement along the width is considered invariant, we have

$$\bar{I}^{(j)} = \mathrm{i}\Omega\frac{\vartheta}{s}\int_{\xi_{j-1}}^{\xi_j}\bar{D}_z\,\mathrm{d}\xi. \tag{35}$$

Substitution Eq. (35) into Eq. (33) yields

$$\bar{I} = \mathrm{i}\Omega\frac{\vartheta}{s}\int_0^{\xi_1}\bar{D}_z\,\mathrm{d}\xi + \mathrm{i}\Omega\frac{\vartheta}{s}\int_{\xi_1}^{\xi_2}\bar{D}_z\,\mathrm{d}\xi + \cdots + \mathrm{i}\Omega\frac{\vartheta}{s}\int_{\xi_{L-1}}^{1}\bar{D}_z\,\mathrm{d}\xi = \mathrm{i}\Omega\frac{\vartheta}{s}\int_0^1\bar{D}_z\,\mathrm{d}\xi. \tag{36}$$

The electric displacement of the top surface of the piezoelectric layer $\bar{D}_Z$ can be obtained from the analysis presented in the previous sections. In the paper, the equipotential surfaces are always assumed at the two sides of the piezoelectric layer. Thus, the dimensionless electric voltage should be

$$\bar{V} = \bar{\phi}_1 - \bar{\phi}_0, \tag{37}$$

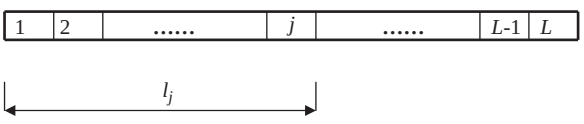

Fig. 2. Divided segments for the piezoelectric layer.

where $\bar{\phi}_1$ is the driven electric potential and $\bar{\phi}_0$ can be derived from Eqs. (23) and (30) for two different cases, respectively. Finally, the admittance of the structural system can be expressed by

$$\bar{Y} = \frac{\bar{I}}{\bar{V}} = \frac{\mathrm{i}\Omega\vartheta \int_0^1 \bar{D}_z \,\mathrm{d}\xi}{(\bar{\phi}_1 - \bar{\phi}_0)s}. \tag{38}$$

Obviously, the dimensionless admittance $\bar{Y}$ contains the information of the interfacial properties and other structural system parameters.

5. Numerical simulations

A three-layered elastic laminate bonded with a piezoelectric layer at the bottom surface of the composite beam is considered. The material properties of the piezoelectric layer and elastic layer [29] are listed in Tables 1 and 2, respectively. The thickness ratio between the four layers is 0.1:0.3:0.3:0.3 (from the bottom layer to the top layer). The width-to-thickness ratio ϑ is 0.2. In addition, the mechanical and dielectric loss factors are taken to be 0.03 and 0.0185 for EM admittance calculation, respectively. In all examples to be considered, we assume $R_z^{(k)} = 0$ to avoid the material penetration phenomenon [30] and take $\bar{R}_x^{(k)} = R^{(k)}$ for simplicity. The following non-dimensional quantities are then introduced:

$$\phi_0 = \frac{\phi}{h}\sqrt{\frac{\bar{\varepsilon}_{33}^{(1)}}{\bar{c}_{11}^{(1)}}}, \quad Y_0 = \frac{Y}{\omega \bar{\varepsilon}_{33}^{(1)} h}, \tag{39}$$

where $Y_0 = G_0 + B_0\mathrm{i}$ and G_0 and B_0 are the real and imaginary parts of the electric admittance, respectively.

To validate EMI model presented here, numerical results are compared with theoretical predications. If the free vibration problem is taken into account, the electrical load is usually assumed to be zero. In this case, the right-hand side of Eq. (25) or Eq. (32) vanishes and the existence of nontrivial solution demands

$$\begin{vmatrix} \mathbf{T}_{21} & \mathbf{T}_{24} \\ \mathbf{T}_{31} & \mathbf{T}_{34} \end{vmatrix} = 0, \tag{40}$$

which gives the frequency equation. The lowest natural frequency parameters $\Omega = \omega h\sqrt{\rho^{(p)}/\bar{c}_{11}^{(p)}}$ of the simply supported laminate for various thickness-to-length ratios and the dimensionless compliance coefficients $R^{(2)}$ are listed in Table 3. In this case, the interface at $\zeta = 0.4$ is assumed to be imperfect while the ones at $\zeta = 0.1$ and 0.7 are perfect.

Then, a uniform electrical load with $\bar{\phi}_1 = 1$ is assumed to be applied on the top surface of the piezoelectric layer. The EM conductance G_0 (the real part of the admittance) signatures obtained by the present EMI method for the same case are

Table 1
Material properties of PZT-4 (transversely isotropic) [29].

Density (kg/m^3)	$\rho = 7500$
Elastic constants ($\times 10^{10}$ N/m^2)	$c_{11} = 13.9$, $c_{12} = 7.8$, $c_{13} = 1.4$, $c_{33} = 33.64$, $c_{44} = 16.25$
Piezoelectric constants (C/m^2)	$e_{15} = 12.7$, $e_{31} = -5.2$, $e_{15} = 15.1$
Dielectric constants ($\times 10^{-11}$ F/m)	$\varepsilon_{11} = 650$, $\varepsilon_{33} = 560$

Table 2
Material properties of an orthotropic elastic material [29].

Density (kg/m^3)	$\rho = 5000$
Elastic constants ($\times 10^{10}$ N/m^2)	$c_{11} = 5.8$, $c_{12} = -5.4$, $c_{13} = 2.3$, $c_{22} = 11$, $c_{23} = 1.3$, $c_{33} = 5.2$, $c_{44} = 1.89$, $c_{55} = 1$, $c_{66} = 3.2$

Table 3
Lowest natural frequency parameter $\Omega = \omega h\sqrt{\rho^{(p)}/\bar{c}_{11}^{(p)}}$ of a simply supported laminate.

h/l	$R^{(2)} = 0$	$R^{(2)} = 0.5$	$R^{(2)} = 1$	$R^{(2)} = 1.5$
0.10	0.018324409	0.018304621	0.018285073	0.018265504
0.15	0.040439534	0.040346866	0.040255051	0.040163975
0.20	0.070086952	0.069820633	0.069558231	0.069299582
0.25	0.106246387	0.105664717	0.105095164	0.104537332
0.30	0.147898045	0.146831214	0.145793472	0.144783699

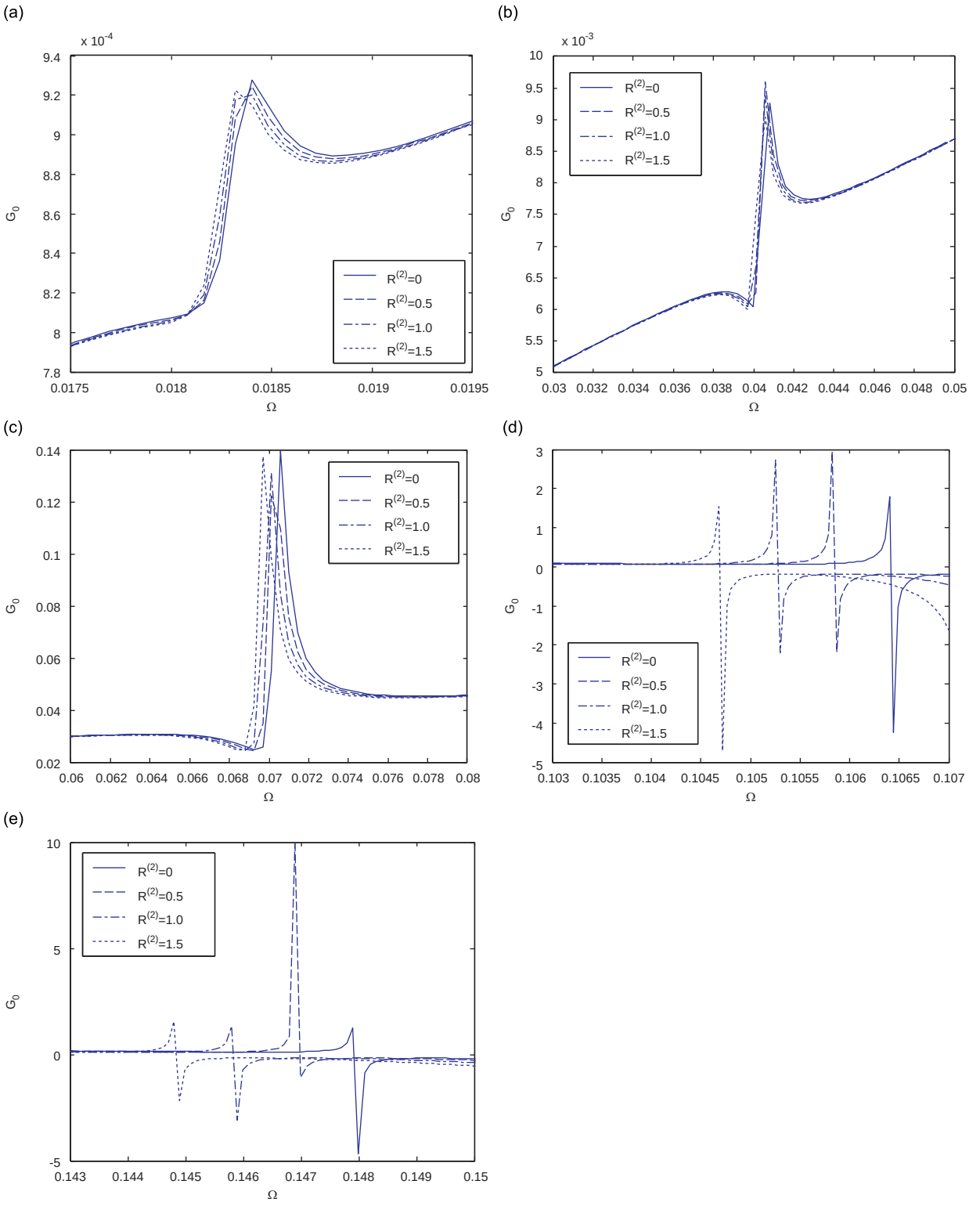

Fig. 3. EM admittance signatures for a laminate in the low frequency range: (a) $h/l = 0.1$; (b) $h/l = 0.15$; (c) $h/l = 0.2$; (d) $h/l = 0.25$; and (e) $h/l = 0.3$.

depicted in Fig. 3. It is shown that the lowest natural frequencies extracted from the EM signatures differ slightly from the numerical results obtained by the frequency equation. For example, in the case of $R^{(2)} = 1$ and $h/l = 0.25$, the error between the numerical results obtained by the two different methods is less than 0.148 percent. Furthermore, as we can see from

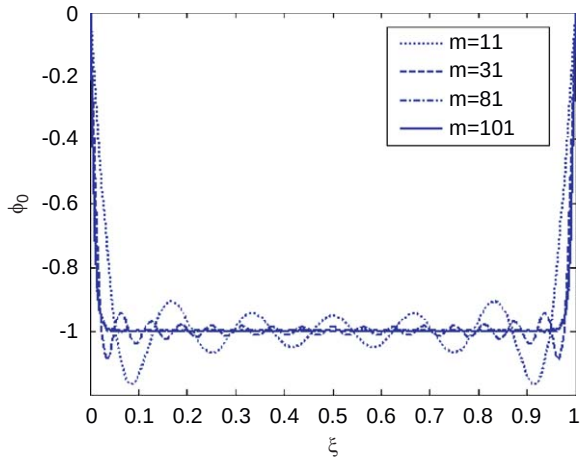

Fig. 4. Distribution of electric potential along the beam length.

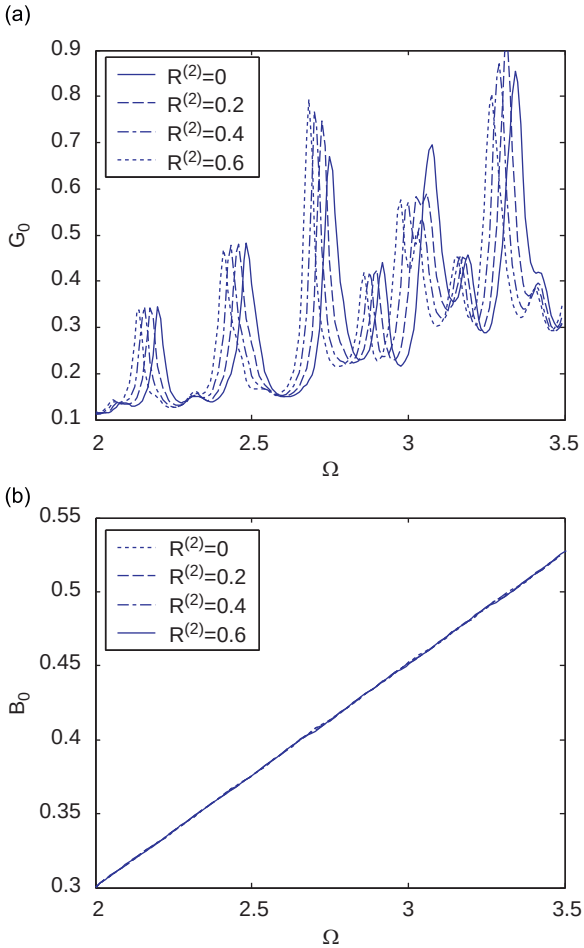

Fig. 5. EM admittance for various interfacial conditions ($\zeta = 0.4$).

Table 3, the more serious the interfacial damage is, the lower the natural frequency will be. That is due to the reduction of the overall stiffness of the laminated beam. The similar trend can also be observed from Fig. 3.

In the following analysis, the thickness-to-length ratio $h/l = 0.1$ is always assumed. As a primary assumption of the present EMI model, the electrode surfaces of the two sides of the piezoelectric transducer are considered to be

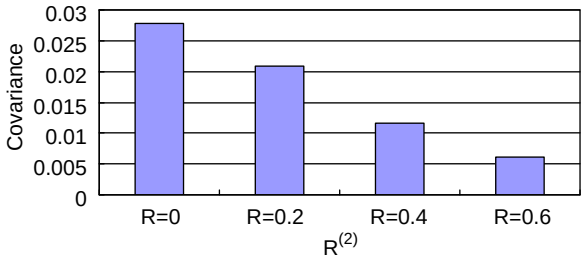

Fig. 6. Covariance versus various interfacial conditions ($\zeta = 0.4$).

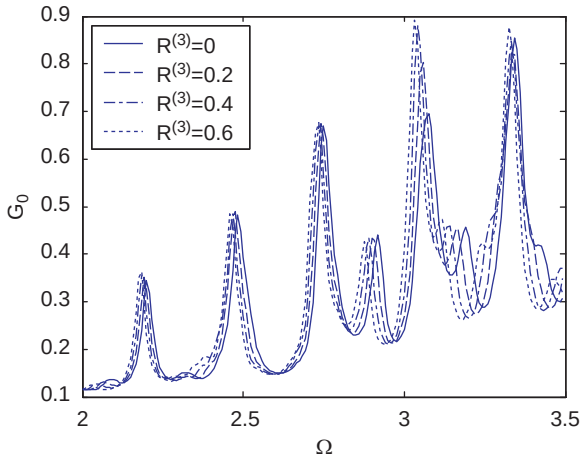

Fig. 7. EM admittance for various interfacial conditions ($\zeta = 0.7$).

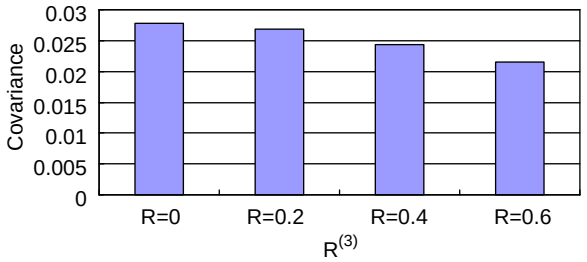

Fig. 8. Covariance versus various interfacial conditions ($\zeta = 0.7$).

equipotential. To check this assumption, the distribution of electric potential along the beam length under a uniform electrical load with $\bar{\phi}_1 = 1$ is displayed in Fig. 4. It is shown that a good precision can be obtained when integer $m = 101$. Also, we can see that the electric potential is almost uniform along the beam length.

The effect of imperfect bonding between the elastic layers on the electric admittance is studied in the higher frequency range. The frequency parameters $\Omega = 2-3.5$ correspond to frequency range 11.35–19.86 kHz, which locates in the typical working frequency range in the EMI technique [31]. Fig. 5(a) shows that the resonant peaks shift towards the left with the increasing compliance coefficient $R^{(2)}$ due to reduction of global stiffness of the composite beam. However, the imaginary part of the admittance seems insensitive to the interfacial defects as shown in Fig. 5(b). The similar observation has been reported in Ref. [23] for a carbon/epoxy laminate bonded with a piezoelectric patch. To quantify changes in the EM admittance signatures, a non-parametric index called covariance, which evaluates the averaged product of deviations of admittance signature data points from their respective means, will be adopted herein. Mathematically, it is defined as [32]

$$\mathrm{Cov} = \frac{1}{N}\sum_{i=1}^{N}(x_i - \bar{x})(y_i - \bar{y}), \tag{41}$$

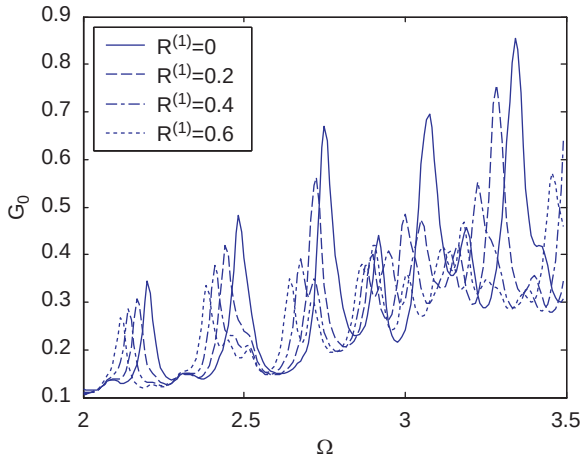

Fig. 9. Effect of imperfect bonding of surface bonded piezoelectric layer on EM signals.

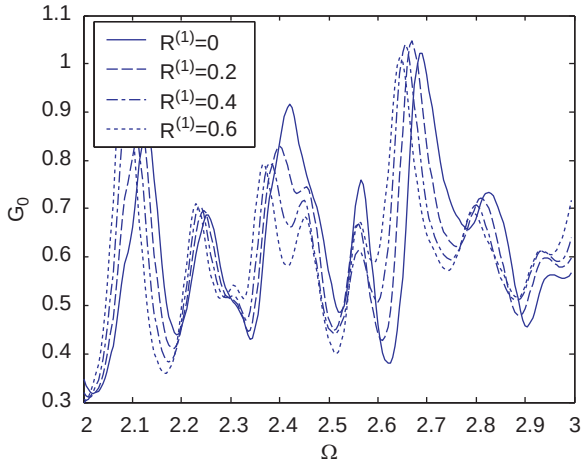

Fig. 10. EM admittance versus various interfacial conditions for a composite beam with an embedded piezoelectric layer ($\zeta = 0.225$).

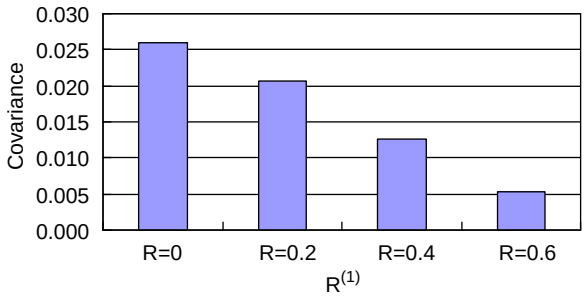

Fig. 11. Covariance versus various interfacial conditions for a composite beam with an embedded piezoelectric layer ($\zeta = 0.225$).

where $\bar{x}$ and $\bar{y}$ are the mean values of two sets of admittance signatures. The more serious the interfacial defect is, the larger deviation between EM admittance signatures appears. This will result in the fact that the covariance index is closer to zero or is negative [32]. As shown in Fig. 6, the covariance values tend closer to zero with aggravating interfacial defects. Although the covariance change is not significant comparing with that obtained in the case of imperfect bonding at $\zeta = 0.4$, a similar trend can also be observed from Figs. 7 and 8 for the case of $\zeta = 0.7$. It can be seen from Fig. 9 that the bonding condition of the sensor/actuator layer also has a significant influence on the output EM signals. Thus, in further research

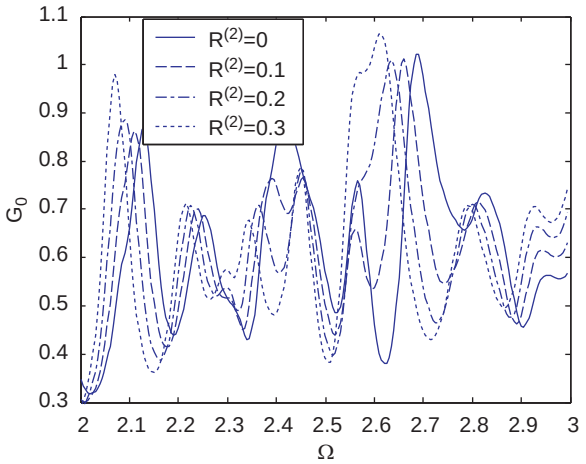

Fig. 12. Effect of imperfect bonding of embedded piezoelectric layer on admittance signals.

and future application of EMI technique, imperfect interfaces between piezoelectric layer and host structures should be taken into account carefully.

A laminated beam composed of an embedded piezoelectric layer (the third layer of the composite) and four identical elastic layers is also investigated. The material properties of the piezoelectric layer and elastic layers including the mechanical and dielectric loss factors are the same as in the first example. The thickness ratio between the five layers is 0.225 : 0.225 : 0.1 : 0.225 : 0.225. The thickness-to-length ratio and the width-to-thickness ratio are 0.1 and 0.2, respectively. A uniform electrical load with $\bar{\phi}_1 = 1$ is applied on the top surface of the piezoelectric layer. From Fig. 10, we can see that the resonant peaks of EM signatures extracted from the embedded piezoelectric layer shift towards the left evidently with aggravating interfacial defects. The covariance index of the impedance signature data indicates a similar phenomenon, as shown in Fig. 11. Furthermore, the effect of imperfect bonding between the piezoelectric transducer and the elastic layer on EM admittance signatures is also displayed in Fig. 12 clearly.

6. Conclusions

This paper considers a surface bonded (and embedded) piezoelectric layer and its interaction with the host laminated beam as a practical model of EMI for composite beams. A spring-layer model is employed to describe the bonding imperfection and an exact analysis based on the state-space formulation is developed. An analytical expression of the electric admittance including the information of the interfacial defects is derived. Comparison with the established method, which employs the frequency equation, validates precision and feasibility of the present analysis.

Numerical results also show that the global stiffness of the composite beam reduces evidently due to the interfacial bonding and the proposed technique can detect the interfacial defects conveniently through monitoring the electro-mechanical admittance signatures. Moreover, it is also shown that the bonding properties of the actuator/sensor layer have great influence on the output electric signal. Thus, attention must be paid to the bonding condition between the piezoelectric layer and the host structure in the field of structural health monitoring using EMI signatures.

In conclusion, the present analysis provides an efficient and convenient technique for investigating the dynamic response of intelligent structure systems in theory. Further, it also provides a powerful, precise and convenient tool to identify the interfacial defects of composite structures quantitatively in practice.

Acknowledgments

The work was sponsored by the National Natural Science Foundation of China (Grant nos. 50778161, 10725210, 10832009), the National Basic Research Program of China (no. 2009CB623204), the Zhejiang Provincial Natural Science Foundation of China (no. Y107796) and K.C. Wong Magna Fund in Ningbo University.

References

[1] D. Montalvão, N.M.M. Maia, A.M.R. Ribeiro, A review of vibration-based structural health monitoring with special emphasis on composite materials, *The Shock and Vibration Digest* 38 (4) (2006) 295–324.

[2] W. Yan, W.Q. Chen, B.S. Wang, On time-dependent behavior of cross-ply laminated strips with viscoelastic interfaces, *Applied Mathematical Modelling* 31 (2007) 381–391.

[3] S.S. Kessler, S.M. Spearing, C. Soutis, Damage detection in composite materials using Lamb wave methods, *Smart Materials and Structures* 11 (2002) 269–278.
[4] R.D. Adams, P. Cawley, C.J. Pye, J. Stone, A vibration testing for non-destructively assessing the integrity of the structures, *Journal of Mechanical Engineering Science* 20 (1978) 93–100.
[5] P. Tan, L. Tong, Identification of delamination in a composite beam using integrated piezoelectric sensor/actuator layer, *Composite Structures* 66 (2004) 391–398.
[6] M. Kisa, Free vibration analysis of a cantilever composite beam with multiple cracks, *Composites Science and Technology* 64 (2004) 1391–1402.
[7] G. Park, H. Sohn, C.R. Farrar, D.J. Inman, Overview of piezoelectric impedance-based health monitoring and path forward, *The Shock and Vibration Digest* 35 (6) (2003) 451–463.
[8] S. Bhalla, C.K. Soh, High frequency piezoelectric signatures for diagnosis of seismic/blast induced structural damages, *NDT & E International* 37 (2004) 23–33.
[9] G. Park, A.C. Rutherford, H. Sohn, C.R. Farrar, An outlier analysis framework for impedance-based structural health monitoring, *Journal of Sound and Vibration* 286 (2005) 229–250.
[10] Y.W. Yang, Y.H. Hu, Electromechanical impedance modeling of PZT transducer for health monitoring of cylindrical shell structures, *Smart Materials and Structures* 17 (2008) 1–11.
[11] C. Bois, C. Hochard, Monitoring of laminated composites delamination based on electro-mechanical impedance measurement, *Journal of Intelligent Material Systems and Structures* 15 (2004) 59–67.
[12] H. Fan, G.F. Wang, Interaction between a screw dislocation and viscoelastic interfaces, *International Journal of Solids and Structures* 40 (2003) 763–776.
[13] J.B. Cai, W.Q. Chen, G.R. Ye, Effect of interlaminar bonding imperfections on the behavior of angle-ply laminated cylindrical panels, *Composites Science and Technology* 64 (2004) 1753–1762.
[14] W.Q. Chen, Y.F. Wang, J.B. Cai, G.R. Ye, Three-dimensional analysis of cross-ply laminated cylindrical panels with weak interfaces, *International Journal of Solids and Structures* 41 (2004) 2429–2446.
[15] N.J. Pagano, Exact solutions for composite laminates in cylindrical bending, *Journal of Composite Materials* 3 (1969) 398–411.
[16] N.J. Pagano, Influence of shear coupling in cylindrical bending of anisotropic laminates, *Journal of Composite Materials* 4 (1970) 330–343.
[17] P. Heyliger, Exact solutions for simply supported laminated piezoelectric plates, *Journal of Applied Mechanics* 64 (1997) 299–306.
[18] L.H. He, J. Jiang, Transient mechanical response of laminated elastic strips with viscous interfaces in cylindrical bending, *Composites Science and Technology* 63 (2003) 821–828.
[19] W. Yan, W.Q. Chen, Time-dependent response of laminated isotropic strips with viscoelastic interfaces, *Journal of Zhejiang University (Science)* 5 (2004) 1318–1321.
[20] J.F. Deü, A. Benjeddou, Free-vibration analysis of laminated plates with embedded shear-mode piezoceramic layers, *International Journal of Solids and Structures* 42 (2005) 2059–2088.
[21] W.Q. Chen, J.P. Jung, K.Y. Lee, Static and dynamic behavior of simply-supported cross-ply laminated piezoelectric cylindrical panels with imperfect bonding, *Composite Structures* 74 (2006) 265–276.
[22] G. Park, C.R. Farrar, F.L.D. Scalea, S. Coccia, Performance assessment and validation of piezoelectric active-sensors in structural health monitoring, *Smart Materials and Structures* 15 (2006) 1673–1683.
[23] C. Bois, P. Herzog, C. Hochard, Monitoring a delamination in a laminated composite beam using in-situ measurements and parametric identification, *Journal of Sound and Vibration* 299 (2007) 786–805.
[24] V.G.M. Annamdas, C.K. Soh, Embedded piezoelectric ceramic transducers in sandwiched beams, *Smart Materials and Structures* 15 (2006) 538–549.
[25] X.P. Qing, S.J. Beard, A. Kumar, T.K. Ooi, F.K. Chang, Built-in sensor network for structural health monitoring of composite structure, *Journal of Intelligent Material System and Structures* 18 (2007) 39–49.
[26] Z.G. Bian, C.W. Lim, W.Q. Chen, On functionally graded beams with integrated surface piezoelectric layers, *Composite Structures* 72 (2006) 339–351.
[27] J. Zhang, B. Zhang, J. Fan, A coupled electromechanical analysis of a piezoelectric layer bonded to an elastic substrate: part I, development of governing equations, *International Journal of Solids and Structures* 40 (2003) 6781–6797.
[28] Y.D. Kuang, G.Q. Li, C.Y. Chen, Dynamic analysis of actuator-driven circular arch or ring using impedance elements, *Smart Materials and Structures* 15 (2006) 869–876.
[29] C.W. Lim, W.Q. Chen, Q.C. Zeng, Exact solution for thick, laminated piezoelectric beams, *Mechanics of Advanced Materials and Structures* 14 (2) (2007) 81–87.
[30] Z.Q. Cheng, A.K. Jemah, F.W. Williams, Theory for multilayered anisotropic plates with weakened interfaces, *Journal of Applied Mechanics* 63 (1996) 1019–1026.
[31] A.S.K. Naidu, C.K. Soh, Damage severity and propagation characterization with admittance signatures of piezo transducers, *Smart Materials and Structures* 13 (2004) 393–403.
[32] W. Yan, C.W. Lim, W.Q. Chen, J.B. Cai, A coupled approach for damage detection of framed structures using piezoelectric signature, *Journal of Sound and Vibration* 307 (2007) 802–817.